Specialty Area: MRI-guided Interventional Therapy

Speaker: Amit Sawant, PhD, Dept. of Radiation Oncology, UT Southwestern Medical Center, Dallas, TX

Highlights

- Effective management of patient motion particularly, respiratory motion, is critical toward ensuring the success of modern thoracic and abdominal radiation therapy
- Rapid MRI has several features that make it an attractive modality for image-guided motion management in radiation therapy
- Many academic groups and industrial vendors are working on integrated MRI + radiotherapy delivery systems
- Current challenges include (i) achieving adequate SNR and spatial resolution which maintaining high acquisition speed (ii) high geometric fidelity in 3D + time for accurate radiotherapy guidance (iii) combining the long-term temporal information from 4D (3D+t) MRI with high spatial resolution and electron density information from 4D computed tomography

Target Audience: Researchers in rapid MRI, interventional radiologists, radiation oncologists

Title: MRI for Motion Management in Radiation Therapy

I. Purpose: The purpose of this talk is to examine the role that rapid MRI can play in the management of patient motion in modern image-guided radiation therapy of thoracic and abdominal tumors.

II. Background

II.A. External beam radiation therapy – Approximately 60 percent of all cancer patients receive some form of radiation therapy (RT) during the course of their treatment. In most cases, modern external-beam RT is administered by gantry-mounted medical linear accelerators (linacs) which accelerate electrons to high energies (6 - 18 MV) in order to generate highly penetrating x-ray beams. Such beams preferentially kill rapidly dividing (i.e., cancerous) cells. The central goal of radiotherapy is to deliver a lethal dose to the tumor target which contains these cancerous cells while, at the same time, minimize radiation damage to surrounding normal tissues and critical organs such as heart, spinal cord, esophagus, etc. For this reason, linacs deliver radiation dose from several angles, termed as "fields" (typically, 3 - 12), such that the beam trajectories intersect at the tumor target and the dose to normal tissues is dispersed over a larger portion of the irradiated volume. In addition, radiation is administered over several daily sessions or "fractions" - typically 25 - 35 so as to limit radiation damage to normal structures. More recently, guided by strong clinical evidence and enabled by technological developments, there has been a trend of “hypo-fractionation”, i.e., delivering the prescribed dose in much fewer fractions. One of the most clinically effective forms of this technique has been stereotactic body radiotherapy (SBRT),

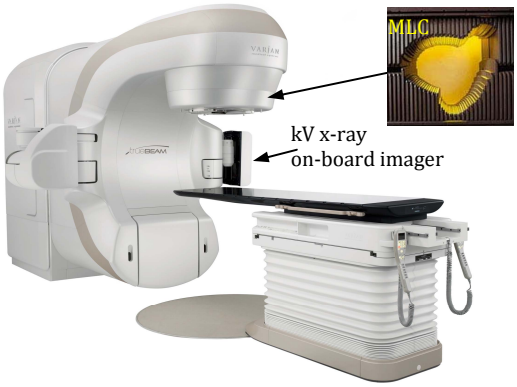

Figure 1. A modern medical linear accelerator or linac (Truebeam, Varian Medical Systems, Palo Alto). The linac is equipped with a 120-leaf multileaf collimator (MLC) to shape each radiation field and an orthogonally-mounted kV x-ray on-board imager (OBI) for patient positioning and monitoring.

also called stereotactic ablative radiotherapy (SABR), which uses sophisticated image-guidance to precisely and accurately deliver high, potent radiation doses in very few (1 – 5) fractions.

II.B. Motion management in thoracic and abdominal RT – Despite these tremendous scientific and technological advances, accurate dose delivery to thoracic and abdominal tumors remains one of the weakest aspects of radiotherapy due to the presence of motion during beam delivery, often termed as intra-fraction motion. Intrafraction deviations occur due to physiological processes (e.g., respiration, bladder filling) or patient-initiated motion (e.g., coughing). For thoracic and abdominal tumors, respiratory motion accounts for the largest intrafraction excursions of the tumor target,[1] causing significant uncertainties in geometric and dosimetric accuracy.[1-3] It follows that the impact of such motion-related uncertainties is amplified in hypofractionated regimens such as SBRT.

Over the last decade, a variety of techniques have been investigated, and many clinically deployed, for managing intrafraction motion. These can be classified into pre-treatment imaging to characterize patient motion (and use the information to create a treatment plan), and in-room imaging to capture real-time motion-related positional variations during beam delivery. Pre-treatment imaging for motion management typically consists of acquiring a respiratory-correlated four dimensional computed tomography scan (4DCT). In this technique, CT projections are acquired over several respiratory cycles and then sorted into 8-10 volumes using a respiratory amplitude trace from an external surrogate marker (optical reflective markers or abdominal pressure belt), to form a single average respiratory cycle[4-6] The main limitation of the 4DCT technique is that respiratory motion is much more complex than can be characterized by a single cycle. Such cycle-to-cycle complexities are unaccounted for in a single-cycle 4D CT and can lead to image artifacts and geometric errors in treatment delivery.[7, 8]

In-room, real-time monitoring of patient position is performed using externally-placed or internally implanted surrogate markers, optical surface photogrammetry systems (an optical grid or speckle pattern is projected on the thoraco-abdominal surface and imaged at a high temporal frequency), x-ray fluoroscopic imaging using kV or MV xrays, or hybrid approaches based on high temporal frequency imaging of external surrogates combined with intermittent imaging of implanted markers using x-ray fluoroscopy. For a comprehensive review on this topic, the reader is referred to the AAPM Task Group 76 report on the management of respiratory motion.[1] Current in-room real-time motion monitoring techniques are limited because they:

i) assume that surrogates consistently and accurately represent internal target motion,
ii) usually monitor only the target centroid for a single target ignoring the interplay between the tumor target and surrounding normal organs and,
iii) impose a patient "cost" due to increased imaging dose and/or interventional complications.

III. MRI-guided motion management for radiotherapy

Several groups including ours are investigating the possibilities of incorporating rapid 2D+t and 3D+t MRI in the image-guided radiotherapy motion management workflow. Plathow *et al.* have reported cine-2D imaging of lung cancer patients at ~3 frames per second (fps),[9] and 4D imaging of malignant pleural mesothelioma patients at ~1 volume/s,[10] under slow-breathing conditions using a 1.5 T scanner. von Siebenthal et al. have reported on a 4D MR imaging technique using retrospective stacking of cine-2D slices.[11] Biederer et al. report 4D MRI of a ventilated chest phantom that uses porcine lung with embedded agarose nodules to simulate tumors.[12] Cai et al. have reported a 4D MRI study of a moving phantom using a technique that uses retrospective sorting of cine-2D slices.[13] Sawant et al., reported rapid 2D +t and 3D + t (4D) MRI of two non-small-cell lung cancer patients to characterize cycle-to-cycle variations and tumor rotation and deformation due to respiratory motion.[14]

III.A. Attractive features of MRI – MRI-based motion management has some very attractive attributes:

i. *No imaging dose* — The absence of ionizing radiation in MRI enables more frequent and longer term monitoring over multiple respiratory cycles, giving us more complete insight into respiratory motion.

ii. *More contrast mechanisms* — MRI allows for a wider variety of intrinsic soft-tissue contrast mechanisms.

iii. *Functionally-guided radiotherapy* — MRI also opens up the possibility of incorporating functional information such as regional ventilation and perfusion for better normal/functional tissue sparing.

III. B Imaging requirements for motion management

SNR vs spatiotemporal resolution – The imaging tasks and, therefore, the SNR requirements of MR imaging for radiotherapy guidance are very different from those for diagnostic MRI. All radiotherapy patients have a confirmed, positive cancer diagnosis. Therefore, compared to the more challenging tasks of diagnosis and tumor classification, the task in image-guided radiotherapy is simpler — boundary detection of the target and/or surrounding anatomy. Thus, we can afford to increase the acquisition speed at the cost of significant SNR degradation and still provide useful image-guidance for the task of motion management.

Geometric fidelity – A critical requirement of image-based guidance is the geometric accuracy in absolute coordinates (e.g., room coordinates). This requirement is different from diagnostic MRI where errors of a few mm may be tolerated in favor of obtaining high SNR. Spatial distortions in MR images can be classified as (i) system-related – due to inhomogeneities in the primary field and/or gradients, (ii) motion-related., and iii) patient-related – due to localized anatomical variations in susceptibility, chemical shift artifacts, etc. For accurate guidance it is important to account and correct for such distortions to within 1 mm accuracy. Various strategies have been proposed to correct for spatial distortions based on the imaging of 3D geometric phantoms or using mutual information (for types i and ii),[15-20] and modeling or measuring susceptibility variations (type iii).[21-24]

III.C Rapid MR imaging — Rapid lung MRI studies have been reported by several groups.[9-12, 25, 26] As a feasibility study, we imaged two NSCLC patients (free-breathing, no extrinsic contrast) on a 1.5T MRI scanner using a balanced steady-state free-precession (bSSFP) sequence (TE/TR: 1.68/3.16 ms; voxel: 2.4 x 3 x 5 mm^3).[27-29] The tumor and diaphragm are clearly seen (Figs. 2a,

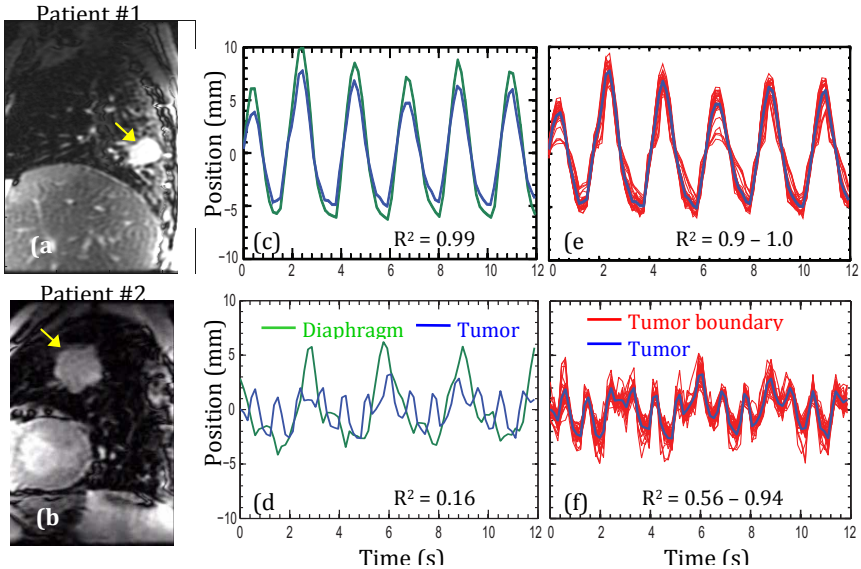

Figure 2. Sagittal MRI of two NSCLC patients using a b-SSFP sequence (T_{acq} = 152 ms). **(a)** Patient#1 with an ~40 mm diameter tumor (yellow arrow) and **(b)** Patient#2 with an ~60 mm diameter tumor (yellow arrow). **(c)** and **(d)** Motion trajectories of the tumor centroid and the dome of the diaphragm for Patient#1 and Patient#2, respectively. **(e)** and **(f)** Trajectories of the tumor centroid and ~15 points on the tumor boundary for Patient #1 and Patient#2, respectively.

b). Acquisition time per frame was 152 ms. For Patient#1, the motion of the tumor centroid was well-correlated with that of the diaphragm (Fig. 2c) and of the tumor boundary (Fig. 2e). However, for Patient#2, these correlations were relatively poor (Figs. 2d, 2f); likely due to the proximity of the cardiac wall. The results from Patient#2 show the importance of long-term imaging to capture cycle-to-cycle effects.

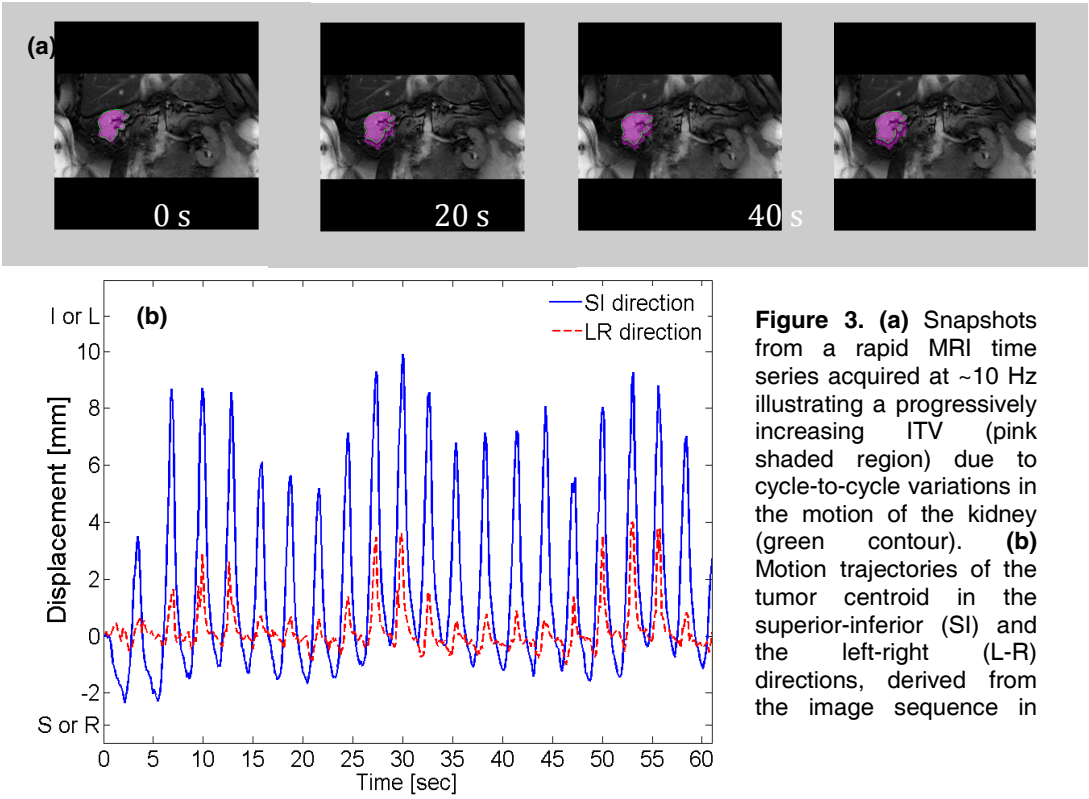

Figure 3. (a) Snapshots from a rapid MRI time series acquired at ~10 Hz illustrating a progressively increasing ITV (pink shaded region) due to cycle-to-cycle variations in the motion of the kidney (green contour). **(b)** Motion trajectories of the tumor centroid in the superior-inferior (SI) and the left-right (L-R) directions, derived from the image sequence in

A highly attractive strategy for further increasing the speed of acquisition is to use sparse-sampling and reconstruction sequences. Figure 3 shows the use of k-t BLAST (2D+t) acquisition at 10 frames/s MRI (1.5T, slice=10mm, resolution= 1.5 x 2 mm2), to image kidney motion over several breathing cycles. The pink region shows the area which the kidney has traversed over at various time points. The fact that the pink region keeps growing from 0 to 60 s suggests the need for long-term monitoring, beyond the single-cycle to generate a more realistic internal target volume (ITV), which is used to define a motion-inclusive target in radiation therapy. In the current conventional 4DCT paradigm, the ITV would be generated using only 1 average respiratory cycle, thereby significantly underestimating the extent of motion. Significant cycle to cycle variations can be observed in the motion trajectories shown in Fig. 3b, e.g., The maximum extent of kidney motion is ~1.2 cm and the variations in peak inhale have a range of ~6 mm. Similarly, while the L-R motion is mostly insignificant, there are instances of large excursions, e.g., around the 50 s mark.

III.D. Integrated MRI+ radiation delivery systems – With a view of achieving the ultimate non-invasive, dose-free, soft-tissue, real-time image guidance, several groups are actively pursuing integrated systems which combine an MRI and a radiation delivery system. A system co-developed by the University Medical Center Utrecht, Netherlands and Elekta (Crawlwy, UK) is based on a 1.5 T MRI scanner with a 6 MV linac.[30-34] A second approach, by ViewRay Inc. (Oakwood village, Ohio), uses a 0.3 T MRI scanner integrated with three Co-60 sources.[35] This system is currently FDA-approved and to date, installed at two sites – Washington University,

St. Louis, MO and UCLA, CA. A related theoretical study from the Peter MacCallum Cancer Centre, Australia involves the integration of a 0.25 T MRI scanner created using two Helmholtz coils coupled with two Co-60 sources in a geometry based on the Tomotherapy system.[36] Finally, a group at the Cross Cancer Institute, University of Alberta, Canada have developed a prototype 0.23 T permanent magnet-based MRI scanner integrated with a 6 MV linac.[37-40]

IV. DISCUSSION AND CONCLUSION

Rapid MRI has tremendous potential in radiotherapy as a valuable tool for motion management. Of course, there are several challenges to address before this goal can be realized clinically. For example, there is much room for exploration of other rapid MRI sequences and for developing sequences specifically optimized for RT guidance. In particular, we expect the largest improvements in imaging speed to come from strategies based on sparse sampling and reconstruction and parallel imaging (e.g., kt-BLAST and k-t SENSE).

Beyond fast imaging, an important and, to date, under-investigated area is developing robust multimodality and multidimensional image registration techniques for the information obtained from rapid MRI (cine-2D or 4D) to be merged with that from 3DCT or 4DCT to create a fused pretreatment 4D image that combines the soft-tissue contrast and temporally dense information from MRI with the spatial accuracy and electron density information from CT. Admittedly, this is a non-trivial problem because one has to account for MRI artifacts, correct for geometric distortions of the anatomy due to the relatively narrow bore of the magnet, and develop robust multimodality image registration tools. However, if these challenges are addressed, fused 4D images would provide a more realistic picture of the behavior of thoracic anatomy over multiple respiratory cycles. Such guidance would enable the development of novel 4D treatment planning paradigms that explicitly account for effects such as baseline shifts, changes in abdominal vs. thoracic breathing, etc. Finally, as discussed in the preceding section, several academic and industrial groups are working on integrated MRI+radiotherapy designs.[31, 39, 41] Online prospective 4D MRI would enable such systems to perform real-time monitoring and, potentially, real-time beam adaptation.

References

1 P.J. Keall, G.S. Mageras, J.M. Balter, R.S. Emery, K.M. Forster, S.B. Jiang, J.M. Kapatoes, D.A. Low, M.J. Murphy, B.R. Murray, C.R. Ramsey, M.B. Van Herk, S.S. Vedam, J.W. Wong, E. Yorke, "The management of respiratory motion in radiation oncology report of AAPM Task Group 76," Medical Physics **33**, 3874-3900 (2006).

2 R. George, P.J. Keall, V.R. Kini, S.S. Vedam, J.V. Siebers, Q. Wu, M.H. Lauterbach, D.W. Arthur, R. Mohan, "Quantifying the effect of intrafraction motion during breast IMRT planning and dose delivery," Medical Physics **30**, 552-562 (2003).

3 G. Hugo, S. Tenn, N. Agazaryan, "An evaluation of intrafraction motion-induced error for fractionated IMRT delivery," Medical Physics **30**, 1470-1470 (2003).

4 G.S. Mageras, A. Pevsner, E.D. Yorke, K.E. Rosenzweig, E.C. Ford, A. Hertanto, S.M. Larson, D.M. Lovelock, Y.E. Erdi, S.A. Nehmeh, J.L. Humm, C.C. Ling, "Measurement of lung tumor motion using respiration-correlated CT," Int J Radiat Oncol Biol Phys **60**, 933-941 (2004).

5 P. Keall, "4-dimensional computed tomography imaging and treatment planning," Seminars in Radiation Oncology **14**, 81-90 (2004).

6 N. Wink, C. Panknin, T.D. Solberg, "Phase versus amplitude sorting of 4D-CT data," J Appl Clin Med Phys **7**, 77-85 (2006).

7 J. Cai, P.W. Read, J.M. Baisden, J.M. Larner, S.H. Benedict, K. Sheng, "Estimation of error in maximal intensity projection-based internal target volume of lung tumors: a simulation and comparison study using dynamic magnetic resonance imaging," Int J Radiat Oncol Biol Phys **69**, 895-902 (2007).

8 J. Cai, P.W. Read, K. Sheng, "The effect of respiratory motion variability and tumor size on the accuracy of average intensity projection from four-dimensional computed tomography: an investigation based on dynamic MRI," Med Phys **35**, 4974-4981 (2008).

[9] C. Plathow, H. Hof, S. Kuhn, M. Puderbach, S. Ley, J. Biederer, C.D. Claussen, P.E. Huber, J. Schaefer, S. Tuengerthal, H.U. Kauczor, "Therapy monitoring using dynamic MRI: analysis of lung motion and intrathoracic tumor mobility before and after radiotherapy," Eur Radiol **16**, 1942-1950 (2006).

[10] C. Plathow, S. Ley, C. Fink, M. Puderbach, W. Hosch, A. Schmahl, J. Debus, H.U. Kauczor, "Analysis of intrathoracic tumor mobility during whole breathing cycle by dynamic MRI," Int J Radiat Oncol Biol Phys **59**, 952-959 (2004).

[11] M. von Siebenthal, G. Szekely, U. Gamper, P. Boesiger, A. Lomax, P. Cattin, "4D MR imaging of respiratory organ motion and its variability," Phys Med Biol **52**, 1547-1564 (2007).

[12] J. Biederer, J. Dinkel, G. Remmert, S. Jetter, S. Nill, T. Moser, R. Bendl, C. Thierfelder, M. Fabel, U. Oelfke, M. Bock, C. Plathow, H. Bolte, T. Welzel, B. Hoffmann, G. Hartmann, W. Schlegel, J. Debus, M. Heller, H.U. Kauczor, "4D-Imaging of the lung: reproducibility of lesion size and displacement on helical CT, MRI, and cone beam CT in a ventilated ex vivo system," Int J Radiat Oncol Biol Phys **73**, 919-926 (2009).

[13] J. Cai, Z. Chang, Z. Wang, W. Paul Segars, F.F. Yin, "Four-dimensional magnetic resonance imaging (4D-MRI) using image-based respiratory surrogate: A feasibility study," Med Phys **38**, 6384 (2011).

[14] A. Sawant, P. Keall, K.B. Pauly, M. Alley, S. Vasanawala, B.W. Loo, Jr., J. Hinkle, S. Joshi, "Investigating the feasibility of rapid MRI for image-guided motion management in lung cancer radiotherapy," BioMed research international **2014**, 485067 (2014).

[15] D. Wang, W. Strugnell, G. Cowin, D.M. Doddrell, R. Slaughter, "Geometric distortion in clinical MRI systems Part I: evaluation using a 3D phantom," Magn Reson Imaging **22**, 1211-1221 (2004).

[16] D. Wang, W. Strugnell, G. Cowin, D.M. Doddrell, R. Slaughter, "Geometric distortion in clinical MRI systems Part II: correction using a 3D phantom," Magn Reson Imaging **22**, 1223-1232 (2004).

[17] T. Mizowaki, Y. Nagata, K. Okajima, R. Murata, M. Yamamoto, M. Kokubo, M. Hiraoka, M. Abe, "Development of an MR simulator: experimental verification of geometric distortion and clinical application," Radiology **199**, 855-860 (1996).

[18] T. Mizowaki, Y. Nagata, K. Okajima, M. Kokubo, Y. Negoro, N. Araki, M. Hiraoka, "Reproducibility of geometric distortion in magnetic resonance imaging based on phantom studies," Radiother Oncol **57**, 237-242 (2000).

[19] T. Stanescu, H.S. Jans, N. Pervez, P. Stavrev, B.G. Fallone, "A study on the magnetic resonance imaging (MRI)-based radiation treatment planning of intracranial lesions," Phys Med Biol **53**, 3579-3593 (2008).

[20] L.N. Baldwin, K. Wachowicz, S.D. Thomas, R. Rivest, B.G. Fallone, "Characterization, prediction, and correction of geometric distortion in 3 T MR images," Med Phys **34**, 388-399 (2007).

[21] C.J. Bakker, M.A. Moerland, R. Bhagwandien, R. Beersma, "Analysis of machine-dependent and object-induced geometric distortion in 2DFT MR imaging," Magn Reson Imaging **10**, 597-608 (1992).

[22] R. Bhagwandien, R. van Ee, R. Beersma, C.J. Bakker, M.A. Moerland, J.J. Lagendijk, "Numerical analysis of the magnetic field for arbitrary magnetic susceptibility distributions in 2D," Magn Reson Imaging **10**, 299-313 (1992).

[23] C.J. Bakker, R. Bhagwandien, M.A. Moerland, L.M. Ramos, "Simulation of susceptibility artifacts in 2D and 3D Fourier transform spin-echo and gradient-echo magnetic resonance imaging," Magn Reson Imaging **12**, 767-774 (1994).

[24] R. Bhagwandien, M.A. Moerland, C.J. Bakker, R. Beersma, J.J. Lagendijk, "Numerical analysis of the magnetic field for arbitrary magnetic susceptibility distributions in 3D," Magn Reson Imaging **12**, 101-107 (1994).

[25] J. Cai, Z. Chang, Z. Wang, W. Segars, F.F. Yin, "Four-dimensional magnetic resonance imaging (4D-MRI) using image-based respiratory surrogate: a feasibility study," Medical Physics **38**, 6384-6394 (2011).

[26] J. Dinkel, C. Hintze, R. Tetzlaff, P.E. Huber, K. Herfarth, J. Debus, H.U. Kauczor, C. Thieke, "4D-MRI analysis of lung tumor motion in patients with hemidiaphragmatic paralysis," Radiother Oncol **91**, 449-454 (2009).

[27] A. Sawant, K. Pauly, M. Alley, S. Vasanawala, B. Loo, S. Joshi, J. Hinkle, P. Keall, "Real-Time MRI for Soft-Tissue-Based IGRT of Moving and Deforming Lung Tumors," Med. Phys. **37**, 3424 (2010).

[28] A. Sawant, Q. Yuan, G. Khatri, S. Joshi, "Rapid MRI for Personalized 4D Image-Guided Lung Cancer Radiotherapy," Med. Phys. **38**, 3770 (2011).

[29] A. Sawant, J. Hinkle, S. Preston, S. Joshi, K.B. Pauly, P. Keall, "Rapid MRI for Real-time Tracking of Rotation/Deformation of Lung Tumors and Organs at Risk," International Journal of Radiation Oncology Biology Physics **78**, S42-S43 (2010).

[30] B.W. Raaymakers, A.J. Raaijmakers, A.N. Kotte, D. Jette, J.J. Lagendijk, "Integrating a MRI scanner with a 6 MV radiotherapy accelerator: dose deposition in a transverse magnetic field," Phys Med Biol **49**, 4109-4118 (2004).

[31] A.J. Raaijmakers, B.W. Raaymakers, J.J. Lagendijk, "Integrating a MRI scanner with a 6 MV radiotherapy accelerator: dose increase at tissue-air interfaces in a lateral magnetic field due to returning electrons," Phys Med Biol **50**, 1363-1376 (2005).

[32] A.J. Raaijmakers, B.W. Raaymakers, S. van der Meer, J.J. Lagendijk, "Integrating a MRI scanner with a 6 MV radiotherapy accelerator: impact of the surface orientation on the entrance and exit dose due to the transverse magnetic field," Phys Med Biol **52**, 929-939 (2007).

[33] A.J. Raaijmakers, B.W. Raaymakers, J.J. Lagendijk, "Experimental verification of magnetic field dose effects for the MRI-accelerator," Phys Med Biol **52**, 4283-4291 (2007).

[34] J.J. Lagendijk, B.W. Raaymakers, A.J. Raaijmakers, J. Overweg, K.J. Brown, E.M. Kerkhof, R.W. van der Put, B. Hardemark, M. van Vulpen, U.A. van der Heide, "MRI/linac integration," Radiother Oncol **86**, 25-29 (2008).

[35] J.F. Dempsey, D. Benoit, J.R. Fitzsimmons, A. Haghighat, J.G. Li, D.A. Low, S. Mutic, J.R. Palta, H.E. Romeijn, G.E. Sjoden, "A Device for Realtime 3D Image-Guided IMRT," Int J Radiat Oncol Biol Phys **63**, S202 (2005).

[36] T. Kron, D. Eyles, J. Schreiner, J. Battista, "Magnetic resonance imaging for adaptive cobalt tomotherapy: A proposal," Journal of Medical Physics **31**, 242-254 (2006).

[37] B. Fallone, M. Carlone, B. Murray, S. Rathee, T. Stanescu, S. Steciw, K. Wachowicz, C. Kirkby, "Development of a Linac-MRI System for Real-Time ART," Medical Physics **34**, 2547 (2007).

[38] B.G. Fallone, M. Carlone, B. Murray, S. Rathee, T. Stanescu, S. Steciw, C. Kirkby, B. Tomanek, J. Sharp, "Development of a small bore linac-MRI system for real time image guided radiotherapy," Radiotherapy and Oncology **84**, S3-S3 (2007).

[39] G. Fallone, M. Carlone, B. Murray, S. Rathee, S. Steciw, "Investigations in the design of a novel Linac-MRI system," International Journal of Radiation Oncology Biology Physics **69**, S19-S19 (2007).

[40] C. Kirkby, T. Stanescu, S. Rathee, M. Carlone, B. Murray, B.G. Fallone, "Patient dosimetry for hybrid MRI-radiotherapy systems," Medical Physics **35**, 1019-1027 (2008).

[41] D.E. Constantin, R. Fahrig, P.J. Keall, "A study of the effect of in-line and perpendicular magnetic fields on beam characteristics of electron guns in medical linear accelerators," Med Phys **38**, 4174-4185 (2011).